Submitted, 2013 Conference on Decision and Control (CDC)
http://www.cds.caltech.edu/~murray/papers/ykm13-cdc.html

Resource Competition as a Source of Non-Minimum Phase Behavior in Transcription-Translation Systems

Enoch Yeung, Jongmin Kim, Richard M. Murray

***Abstract*— In this paper, we explore how resource limitations can lead to coupling interactions between orthogonal components in a transcription-translation system and the effect those interactions have on its dynamical behavior. To illustrate these ideas, we present a motivating example featuring a classical network motif: the signal cascade. We show that through coupling interactions arising from competition for limited resources, the system exhibits a non-minimum phase step response. These observations lead us to identify a key network motif with the potential to introduce right half plane zeros into the system transfer function. We characterize the parametric conditions under which the network motif produces a non-minimum phase transfer function and illustrate with two examples how resource limitations can 1) introduce the network motif through these coupling interactions, 2) satisfy the parametric conditions sufficient to produce a right half plane zero.**

I. Introduction

One of the primary goals of synthetic biology is to manipulate and synthesize novel biochemical devices to achieve an objective. For *in vivo* applications, this often means exploiting the resources available in a host organism. For example, the authors in [1] combine the technology of combinatorial promoters with the native transcription and translation machinery in *E. coli* to achieve robust oscillation. In [2], the authors took advantage of native protein folding machinery and plasmid replication proteins to monitor a low copy number oscillator using GFP expressed on a high copy number plasmid — by so doing, they were able to determine that low copy number gene expression was stochastic. More recently, the authors in [3] take advantage of the clustered regularly interspaced short palindromic repeats (CRISPR) pathway and endoribonucleases to achieve polycistronic transcriptional and translational expression. In each scenario, these synthetic technologies utilize the resources available in a cell to achieve their objective, whether those resources are available in abundance or scarcity.

Substantial experimental work has been done experimentally that indicates resources can be scarce in the cell. In [4], the authors demonstrate that too many LVA-tagged components in a synthetic circuit causes saturation of ClpXP degradation enzyme, creating coupling between originally orthogonal components. They show these coupling interactions are strong enough to destroy the robustness of the oscillator from [1].

On the modeling side, substantial work has been done to quantify both theoretically and empirically the scarcity of resources and the impact it can have on synthetic biocircuit dynamics. The scarcity of resources often leads to unintentional coupling, referred to as retroactivity [5], crosstalk [6], loading effects [7], etc. Strategies for attenuating this crosstalk have been proposed in [8], [5], and [6]. There is ongoing work about how to scale these strategies for larger systems, where multiple components may be subject to retroactivity and there is a limit to the number of heterogenous control strategies that are simultaneously implementable in the system.

Our goal in this paper is complementary to the work in [8], [5], [7]: we seek to understand the effects of resource crosstalk on synthetic circuit performance, specifically the effect that resource crosstalk can have in producing right half plane zeros in the local dynamics of a transcription-translation system about an equilibrium point. A right half plane zero is viewed as a source of fundamental limitations on closed loop performance [9]. Thus, it is important to understand the conditions under which right half plane zeros can arise from resource limitations, and the fundamental limits they impose on synthetic biocircuit performance and naturally occurring regulatory circuits. In addition, our work should be viewed as complementary to the analysis on glycolysis systems, as it considers yet another scenario where right half plane zeros play a role in limiting system performance in biological systems [10].

We organize our paper as follows: in Section II we develop a motivating example system to illustrate how crosstalk interactions can lead to a non-minimum phase transfer function. In Section III we show that a simple network motif plays the primary role in introducing RHP zeros — we present both a motivating example and a generalizing result that characterizes the parametric and functional conditions under which right half plane zeros exist. Next, in Section IV, we apply the results of Section III to identify a general class of transcription-translation systems that have a right half plane zero under certain parametric conditions. Finally, in Section V we show how degradation and ribosomal loading in certain types of synthetic biocircuits can have the potential to introduce a right half plane zero and adversely affect the master stress response of a host *E. coli* cell.

II. Motivation - Resource Limitations in a Signal Cascade

Whether a synthetic biocircuit is implemented *in vivo* or *in vitro*, if it utilizes transcriptional or translational machinery, e.g. NTP, ATP, polymerases, σ-factors, ribosomes, or degrades using shared degradation enzymes, e.g. ribonucleases or proteases, then it has the potential to saturate or overload

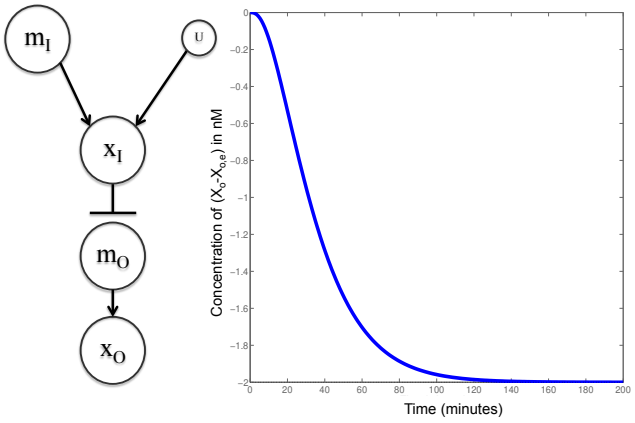

Fig. 1. (Left) An illustration of the signal cascade system (1). The input u upregulates x_I, which subsequently represses expression of the output gene's mRNA m_O. (Right) The step response of the Michaelis-Menten crosstalk-free signal cascade system (1). Parameter values for the simulation were $R_I = R_O = 1.51$ nM/s, $D_I = D_O = 2$ nM/s, $k_{M,I} = 20$ nM, $k_{M,O} = 40$ nM , $\kappa_{M,I} = 3.1$ nM, $\kappa_{M,O} = 2.9$ nM, $\alpha_I = .002$ nM/s, $\alpha_O = .001$ nM/s, $\delta = 0.005$/s, $k_{IU} = 10^{-7}$ /s and $k_{OI} = 625 \times 10^{-9}$ /s. The system's transfer function is minimum phase, since it has three poles in the left half plane of $\mathbb{C}$ and no zeros.

these resource molecules and interfere with other processes in the system. These saturation effects can lead to sequestration of enzymes from critical processes that would otherwise function normally. These sequestration effects are the basis of resource mediated-crosstalk interactions in a system. When these crosstalk interactions are substantial, they can lead to unwanted coupling between otherwise orthogonal processes. It is when that coupling augment the existing network of interactions to form a specific type of network motif that right half plane zeros can arise. To gain intuition let us consider an example system that uses a ubiquitous network motif: the signal cascade.

Let x_O and x_I be two proteins in a signal cascade network translated from mRNA molecules m_O and m_I respectively. Let u be an input (e.g. an inducer or allosteric activator) that activates the cascade via x_I. Suppose that x_I represses expression of mRNA transcript m_O. If expressed, m_O translates to x_O as the final output protein of the cascade. We suppose that the production and degradation of x_O and x_I can be described as Michaelis-Menten functions (without competitive effects). A schematic illustrating the cascade is shown in Figure 1. We write the model for this system as follows:

$$\begin{aligned}
\dot{m}_I &= \alpha_I - \delta m_I \\
\dot{x}_I &= R_I \frac{\frac{m_I}{k_{M,I}}}{1+\frac{m_I}{k_{M,I}}} - D_I \frac{\frac{x_I}{\kappa_{M,I}}}{1+\frac{x_I}{\kappa_{M,I}}} + k_{IU} u \\
\dot{m}_O &= \alpha_O - k_{OI} x_I - \delta m_O \\
\dot{x}_O &= R_O \frac{\frac{m_O}{k_{M,O}}}{1+\frac{m_O}{k_{M,O}}} - D_O \frac{\frac{x_O}{\kappa_{M,O}}}{1+\frac{x_O}{\kappa_{M,O}}} \\
y &= x_O
\end{aligned} \tag{1}$$

Here we have attempted to capture a signal cascade in the simplest possible terms. In doing so, we acknowledge that we have omitted the usual Hill functions that describe transcriptional activation and ignored the intricate processes behind the production of mRNA, including isomerization, strand elongation, fall-off, etc.. Our goal is to capture the essence of the network structure and relationships between states in this signal cascade, but with minimal complexity so that when we add modeling terms to describe resource competition, the introduction of a right half plane zero will be transparent. After linearizing, we compute the transfer function as

$$G(s) = \frac{-\frac{\frac{R_O}{k_{M,O}}}{\left(1+\frac{m_{O,e}}{k_{M,O}}\right)^2} k_{OI} k_{IU}}{(s+\delta)\left(s - \frac{\frac{-D_I}{\kappa_{M,I}}}{(1+\frac{x_{I,e}}{\kappa_{M,I}})^2}\right)\left(s + \frac{\frac{D_O}{\kappa_{M,O}}}{(1+\frac{x_{O,e}}{\kappa_{M,O}})^2}\right)}.$$

Clearly, $G(s)$ has no right half plane zeros, so the system is minimum phase. The step response to a step input is plotted in Figure 1. Now consider a model that incorporates the effects of substrates competing for the same resources. In particular, we will suppose that m_I and m_O compete for the same ribosomes R to translate x_I and x_O respectively and that x_O and x_I compete for the same degradation enzymes D. We write it as follows.

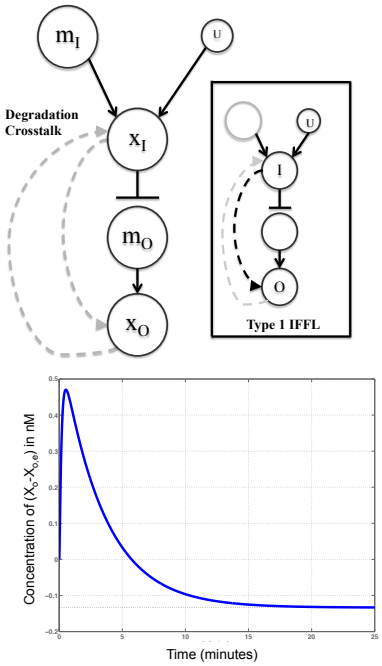

Fig. 2. (Top) An illustration of the signal cascade system (2) including sequestration interactions from degradation enzyme loading. The actual cascade is the same as before: the input u upregulates x_I, which subsequently represses expression of the output gene's mRNA m_O. However, x_I sequesters degradation enzyme from x_O, which has the effect of increasing x_O concentration. Thus, we draw an effective (positive) arrow from x_I to x_O. Similarly, x_O sequesters degradation enzyme from x_I so we draw a (positive) arrow from x_O to x_I. In particular, one of the crosstalk edges introduces a Type I incoherent feedforward loop into the system (see inset). (Bottom) The step response of the linearization of system (2) is plotted here. The transfer function is now non-minimum phase with right half plane zero $z = 0.0012$. Parameter values were chosen so that $R = R_I = R_O$, $D = D_I = D_O$ and all other parameters are the same as in Figure 1.

$$\begin{aligned}
\dot{m}_I &= \alpha_I - \delta m_I \\
\dot{x}_I &= \frac{R\frac{m_I}{k_{M,I}}}{1+\frac{m_I}{k_{M,I}}+\frac{m_O}{k_{M,O}}} - \frac{D\frac{x_I}{\kappa_{M,I}}}{1+\frac{x_I}{\kappa_{M,I}}+\frac{x_O}{\kappa_{M,O}}} + k_{IU}u \\
\dot{m}_O &= \alpha_O - k_{OI}x_I - \delta m_O \\
\dot{x}_O &= \frac{R\frac{m_O}{k_{M,O}}}{1+\frac{m_O}{k_{M,O}}+\frac{m_I}{k_{M,I}}} - \frac{D\frac{x_O}{\kappa_{M,O}}}{1+\frac{x_O}{\kappa_{M,O}}+\frac{x_I}{\kappa_{M,I}}} \\
y &= x_O
\end{aligned} \tag{2}$$

and the linearized system is of the form

$$\begin{bmatrix} -\delta & 0 & 0 & 0 \\ a_{21} & a_{22} & a_{23} & a_{24} \\ 0 & -k_{OI} & -\delta & 0 \\ a_{41} & a_{42} & a_{43} & a_{44} \end{bmatrix}, \tag{3}$$

where

$$\begin{aligned}
a_{21} &= \frac{\frac{R}{k_{M,I}}(1+\frac{m_{O,e}}{k_{M,O}})}{(1+\frac{m_{I,e}}{K_{M,I}}+\frac{m_{O,e}}{K_{M,O}})^2},\ a_{41} = \frac{-\frac{R}{K_{M,I}}(\frac{m_{O,e}}{K_{M,O}})}{(1+\frac{m_{I,e}}{k_{M,I}}+\frac{m_{O,e}}{k_{M,O}})^2} \\
a_{22} &= \frac{\frac{-D}{\kappa_{M,I}}(1+\frac{x_{O,e}}{\kappa_{M,O}})}{(1+\frac{x_{I,e}}{\kappa_{M,I}}+\frac{x_{O,e}}{\kappa_{M,O}})^2},\ a_{42} = \frac{\frac{D}{\kappa_{M,I}}\frac{x_{O,e}}{\kappa_{M,O}}}{(1+\frac{x_{I,e}}{\kappa_{M,I}}+\frac{x_{O,e}}{\kappa_{M,O}})^2} \\
a_{23} &= \frac{-\frac{R}{k_{M,O}}(\frac{m_{I,e}}{k_{M,I}})}{(1+\frac{m_{I,e}}{k_{M,I}}+\frac{m_{O,e}}{k_{M,O}})^2},\ a_{43} = \frac{\frac{R}{k_{M,O}}(1+\frac{m_{I,e}}{k_{M,I}})}{(1+\frac{m_{I,e}}{k_{M,I}}+\frac{m_{O,e}}{k_{M,O}})^2} \\
a_{24} &= \frac{\frac{D}{\kappa_{M,O}}\frac{x_{I,e}}{\kappa_{M,I}}}{(1+\frac{x_{I,e}}{\kappa_{M,I}}+\frac{x_{O,e}}{\kappa_{M,O}})^2},\ a_{44} = \frac{\frac{-D}{\kappa_{M,O}}(1+\frac{x_{I,e}}{\kappa_{M,I}})}{(1+\frac{x_{I,e}}{\kappa_{M,I}}+\frac{x_{O,e}}{\kappa_{M,O}})^2}.
\end{aligned} \tag{4}$$

and $B = k_{IU}\mathbf{e_2}$ and $C = \mathbf{e_4}^T$, where $\mathbf{e}_i$ denotes the i^{th} standard basis vector. We then have

$$G(s) = \frac{(a_{42}k_{IU})s - a_{43}k_{OI}k_{IU} + a_{42}\delta k_{IU}}{D(s)}$$

with characteristic polynomial $D(s) = s^3 - (a_{22}+a_{44}-\delta)s^2 - (a_{24}a_{42} - a_{22}a_{44} + (a_{22}+a_{44})\delta - a_{23}k_{OI})s + a_{22}a_{44}\delta - a_{22}a_{42}\delta - a_{23}a_{43}k_{OI} + a_{24}a_{43}k_{OI}$. With the appropriate constraints on the balance between degradation and production, the poles will lie in the left half plane. However, notice that $G(s)$ has a zero at

$$z = \frac{a_{43}k_{OI}}{a_{42}} - \delta, \tag{5}$$

and since $\delta > 0$, the zero is in the right half plane if the ratio $(a_{43}k_{OI})/a_{42}$ is sufficiently large. The coefficient a_{42} describes how x_I impacts x_O via indirect competition for the limited degradation enzyme. As the amount of x_I at equilibrium increases, a_{42} grows smaller and less x_O is degraded, since the degradation enzymes become more likely to be bound to x_I substrate. However, through the signal cascade, x_I inhibits x_O with effective gain $a_{43}k_{OI}$. As the amount of x_I at equilibrium increases, a_{42} can grow small enough so that $a_{43}k_{OI}/a_{42}$ approaches δ from the right hand side, resulting in a small (slow) right half plane zero which place stronger constraints on the controller. Figure 2 shows the step response for system (2) with a particularly slow right half plane zero.

Notice that if the signal cascade was designed so that x_I activated x_O, then the term $-k_{OI}$ would be replaced with k_{OI} and the zero would be

$$z = -(\frac{a_{43}k_{OI}}{a_{42}} + \delta) < 0. \tag{6}$$

Thus, it appears that the incoherence, or opposing dynamics of 1) x_I repressing x_O and 2) x_I "promoting" the abundance of x_O by saturating degradation enzyme, is necessary to produce a right half plane zero. If the signal cascade is designed so that x_I activates x_O, then the incoherent feedforward loop becomes a coherent feedforward loop and the right half plane zero disappears. It is the incoherent feedforward loop that makes $G(s)$ non-minimum phase; thus the next section focuses on characterizing how and when incoherent feedforward loops produce right half plane zeros in $G(s)$.

III. Analysis of the Incoherent Feedforward Loop Network Motif

In this section, we characterize how RHP zeros arise in incoherent feedforward loops. To acquire intuition, we first pose a simple linear two state model of the incoherent feedforward loop and derive the transfer function for the system. We then show that the transfer function for this incoherent feedforward loop network has a RHP zero and derive the parametric conditions which are sufficient to produce a RHP zero. Next, we generalize the result to single-input single-output (SISO) systems with an arbitrary number of states and show that under certain conditions, incoherence results in a RHP zero. We then conclude this section with an example illustrating the theorem. Consider the following linear two state model for a feedforward loop:

$$\begin{aligned}
\dot{x}_I &= -\delta_I x_I + k_{IU}u \\
\dot{x}_O &= -\delta_O x_O + k_{OI}x_I + k_{OU}u \\
y &= x_O
\end{aligned} \tag{7}$$

The transfer function for this system is

$$G(s) = \frac{k_{OU}s + \delta_I k_{OU} + k_{OI}k_{IU}}{(s+\delta_I)(s+\delta_O)}$$

and has a zero at

$$z = -\left(\frac{k_{OI}k_{IU}}{k_{OU}} + \delta_I\right).$$

Notice the similarity between z here and the zero in equation (6). The feedforward loop is coherent (incoherent) whenever the sign of $k_{OI}k_{IU}$ is the same as (opposite of) the sign of k_{OU}. This condition succinctly characterizes all four types of incoherent feedforward loops and all four types of coherent feedforward loops. In the nonlinear setting, such a succinct characterization may be hard to find, but as our analysis pertains to transfer functions, this condition will suffice for determining if a feedforward loop is incoherent or coherent.

Since δ_I represents a degradation rate for x_I, then $\delta_I > 0$ and the potential for $z > 0$ exists only when

$$\frac{k_{OI}k_{IU}}{k_{OU}} < 0$$

and δ_I small enough. Notice that if we separate the B matrix as

$$B = B_I + B_D = \begin{bmatrix} k_{IU} \\ 0 \end{bmatrix} + \begin{bmatrix} 0 \\ k_{OU} \end{bmatrix}$$

we can decompose the transfer function $G(s)$ as

$$\begin{aligned} G(s) &\equiv G_I(s) + G_D(s) \\ &\equiv C(sI - A)^{-1}B_I + C(sI - A)^{-1}B_D \\ &= \frac{k_{OI}k_{IU}}{(s+\delta_I)(s+\delta_O)} + \frac{k_{OU}}{(s+\delta_O)}, \end{aligned}$$

where $G_I(s)$ represents the transfer function describing dynamics of the feedforward loop from U to the output X_O that requires the intermediate state I and $G_D(s)$ is the transfer function that describes the dynamics of the feedforward loop that go directly from U to X_O.

Viewed this way, we see that the feedforward loop transfer function $G(s)$ has a right half plane zero when the gain of $G_I(s)$ has opposite sign of the gain of $G_D(s)$, i.e. the two modes are incoherent, and the gain of $G_I(s)$ is sufficiently larger than the gain of $G_D(s)$. The two transfer functions capture the dynamics of the two pathways for controlling X_O. When those pathways are incoherent and the gain of the pathway with an intermediate state (i.e. the slower pathway) is sufficiently large, then the step response $G(s)$ is temporarily dominated by $G_D(s)$ since $G_I(s)$ must integrate one state before the signal propagates to x_O. The result is a transient consistent with the sign of the gain of $G_D(s)$. However, in the long run, $G_I(s)$ dominates the dynamics of $G(s)$ since the gain of $G_I(s)$ is larger, resulting in convergence to steady state in a direction opposite the initial transient driven by $G_D(s)$. These dynamics are a direct consequence of the structure of the incoherent feedforward loop. The incoherent feedforward loop thus yields structural intuition into the characteristic inverse step response observed for a non-minimum phase SISO transfer function with a single RHP zero.

In general, biological systems possess many states and potentially many feedforward loops embedded in a single network. Moreover, the location of the input and the placement of the reporter molecule, i.e. the output of the system, play a key role in determining if a feedforward loop even exists between the input and the output. This is consistent with classical examples of non-minimum phase systems; sensor placement relative to actuator location can make all the difference in eliminating a right half plane zero. [9]. If a feedforward loop exists, there may be several and in particular, the sequestration effects of resource loading (e.g. ribosomes, polymerases, transcription factors, ribonucleases, proteases, shared metabolic enzymes) may result in additional feedforward loops that were not included in the designed or natural system. If multiple feedforward loops are present, then it is critical to determine what the overall dominant or 'net' feedforward loop is, and whether it is incoherent or coherent. Typically, the model for a multi-state transcription-translation system, when considering the local dynamics about an equilibrium point, can be approximated with a linear time-invariant state space realization.

However, it is not easy to determine the existence of a incoherent feedforward loop at first glance from the state-space realization. Often, it is easier to consider a candidate intermediate node x_I and the output node x_O in the network and ask if there is an *effective* incoherent feedforward loop in the system. In this scenario, it would be useful to find a simpler representation of system structure that embeds the dynamics of unnecessary intermediate states as open loop transfer functions and describes the overall effect of u on x_I, x_I on x_O, and u on x_O. The dynamical structure function [11] is a convenient representation of structure that has this property. We develop the following lemma, based on the techniques in [11].

Lemma 1: Consider the system

$$\dot{z} = Az + Bu \tag{8}$$

$$y = \begin{bmatrix} c & 0 \end{bmatrix} z \tag{9}$$

where $z = \begin{bmatrix} x_O & x_I & x^T \end{bmatrix}^T$, $x_O(t), x_I(t) \in \mathbb{R}$ for all t, $x(t) \in \mathbb{R}^{n-2}$ for all t, $A \in \mathbb{R}^{n\times n}, B \in \mathbb{R}^n, c \in \mathbb{R}, C \in \mathbb{R}^{1\times n}$. Then the system can be expressed as

$$\begin{bmatrix} sX_O(s) \\ sX_I(s) \end{bmatrix} = \begin{bmatrix} W_{OO}(s) & W_{OI}(s) \\ W_{IO}(s) & W_{II}(s) \end{bmatrix} \begin{bmatrix} X_O(s) \\ X_I(s) \end{bmatrix} + \begin{bmatrix} V_O(s) \\ V_I(s) \end{bmatrix} U(s) \tag{10}$$

where $W_{OI}(s)$ is a transfer function describing the open loop dynamics from $X_I(s)$ to $X_O(s)$ involving only the states in $X(s)$ (excluding $X_I(s)$ and $X_O(s)$), $W_{OO}(s)$ is a transfer function describing self-regulatory open loop dynamics of X_O that involve only states in $X(s)$, $V_O(s)$ is the open loop transfer function from U to X_O describing dynamics that involve only states in $X(s)$, etc.

Proof: Observing the partitioning in the state vector $z = \begin{bmatrix} x_O & x_I & x^T \end{bmatrix}^T$, we can write state space equation matrices in block form as:

$$\begin{aligned} \begin{bmatrix} \dot{x_O} \\ \dot{x_I} \\ \dot{x} \end{bmatrix} &= \begin{bmatrix} A_{11} & A_{12} & A_{13} \\ A_{21} & A_{22} & A_{23} \\ A_{31} & A_{32} & A_{33} \end{bmatrix} \begin{bmatrix} x_O \\ x_I \\ x \end{bmatrix} + \begin{bmatrix} B_1 \\ B_2 \\ B_3 \end{bmatrix} u \\ y &= cx_O + \begin{bmatrix} 0 \end{bmatrix} x = cx_O \end{aligned} \tag{11}$$

Assuming $X(0) = 0$, we take Laplace transforms and solve for $X(s)$ in the third row to obtain

$$X(s) = (sI - A_{33})^{-1} \left(\begin{bmatrix} A_{31} & A_{32} \end{bmatrix} \begin{bmatrix} X_O(s) \\ X_I(s) \end{bmatrix} + B_3 U(s) \right),$$

and noting that $(sI - A_{33})^{-1}$ exists almost everywhere on $\mathbb{C}$, substituting this expression for $X(S)$ results in

$$\begin{bmatrix} sX_O(s) \\ sX_I(s) \end{bmatrix} = \begin{bmatrix} W_{OO}(s) & W_{OI}(s) \\ W_{IO}(s) & W_{II}(s) \end{bmatrix} \begin{bmatrix} X_O(s) \\ X_I(s) \end{bmatrix} + \begin{bmatrix} V_O(s) \\ V_I(s) \end{bmatrix} U(s),$$

where

$$\begin{aligned} W_{OO}(s) &= A_{11} + A_{13}(sI - A_{33})^{-1}A_{31}, \\ W_{OI}(s) &= A_{12} + A_{13}(sI - A_{33})^{-1}A_{32}, \\ W_{IO}(s) &= A_{21} + A_{23}(sI - A_{33})^{-1}A_{31}, \\ W_{II}(s) &= A_{22} + A_{23}(sI - A_{33})^{-1}A_{32}, \\ V_O(s) &= B_1 + A_{13}(sI - A_{33})^{-1}B_3, \\ V_I(s) &= B_2 + A_{23}(sI - A_{33})^{-1}B_3. \end{aligned} \tag{12}$$

■

This lemma shows that an arbitrary state space realization can be used to compute the open loop (proper) transfer functions describing the relationships between the output state x_O, intermediate x_I and input u. Notice that the form of equation (10) resembles the form of system (7); immediately, the question arises if the findings in the prequel generalize to transfer functions. The next result answers this question:

Theorem 1: Suppose the system (8) is asymptotically stable. Suppose, for all $x \in \mathbb{R}_{\geq 0}$ we have that

$$\left(\frac{W_{OI}(x)V_I(x)}{V_O(x)}\right) \leq 0 \text{ and } W_{II}(x) \geq \left(\frac{W_{OI}(x)V_I(x)}{V_O(x)}\right)$$

for all $x \in \mathbb{R}_{\geq 0} \subset \mathbb{C}_{\geq 0}$. Further, if

$$W_{II}(s) - \frac{W_{OI}(s)V_I(s)}{V_O(s)} = k(s+D) + f_p(s),$$

where $0 \leq k < 1, D \in \mathbb{R}$ and $f_p(s)$ is a proper transfer function, then the transfer function of system (8) has at least one zero z in the closed right half plane of $\mathbb{C}$. Moreover, z is a nonnegative real number.

Proof: Let the set of nonnegative real numbers be denoted as X. Define $f(s) = W_{II}(s) - \frac{W_{OI}(s)V_I(s)}{V_O(s)}$. After some algebra, the transfer function of the system can written as

$$G(s) = \frac{s - f(s)}{((s - W_{OO}(s))(s - W_{II}(s)) - W_{OI}W_{IO})}.$$

To show $G(s)$ has at least one zero in X, it suffices to show that $x - f(x)$ has a root $z \in X$. Since $\frac{W_{OI}(x)V_I(x)}{V_O(x)} \leq 0$ and $W_{II}(x) \geq \frac{W_{OI}(x)V_I(x)}{V_O(x)}$, then $f(x) \geq 0$ for all $x \in X$. Since the system is asymptotically stable, this implies that $f(x)$ has no right half plane poles in X. Define $p(x) = x - f(x) = x - (k(x+D) + f_p(x))$; clearly $p(x)$ is continuous since $f(x)$ has no poles in X. Notice that $p(0) = -f(0)$. If $f(0) = 0$, then we are done. If $f(0) \neq 0$, then $f(0) > 0$ which implies $p(0) < 0$. Next, write $p(x) = (1-k)x - kD - f_p(x)$. Since $f_p(x)$ is proper, it is globally bounded on X. Denote

$$M = \max\{\sup_{x \in X} f_p(x), |kD|\}.$$

Then if $x > (M + kD)/(1-k)$, $p(x) > 0$ and by continuity of $p(x)$ and the intermediate value theorem, $p(z) = 0$ for some $z \in X$. ∎

Remark 1: The constraint that $f(x)$ be at least relative degree -1 can be interpreted as a constraint on the structure of the system (8). Since $W_{II}(s)$ is either proper or strictly proper, the improperness of $f(x)$ can only arise from the ratio $\frac{W_{OI}(x)V_I(x)}{V_O(x)}$ being improper. Since $W_{OI}(x)$ and $V_I(x)$ are proper, again, the only way that the ratio is improper is if $V_O(x)$ is strictly proper. When $V_O(x)$ has relative degree 0, then the $f(x)$ has relative degree 0, when $V_O(x)$ has relative degree one, then $f(x)$ has relative degree -1, and so forth. Thus, the constraint on $V_O(x)$ is that it possesses direct feedthrough from u to x_O (relative degree 0), or that there is effectively at most one integrator from u to x_O (relative degree 1).

Remark 2: The condition that $f(x) \geq 0$ for all $x \in X$ can be viewed as a constraint on the zeros of $f(x)$. Since the poles of $f(x)$ all lie in the open left half plane, $f(x)$ can never have a negative denominator. Therefore, to ensure that $f(x) > 0$ for all $x \in X$, any right half plane zero in $f(x)$ must have even algebraic multiplicity.

IV. Input-Coupled Systems

We now consider a general class of transcriptional and translational systems, comprised of at least two orthogonal genes. We suppose these two genes are activated by a small input molecule u_1 and thus refer to this type of system as an input-coupled system. The model is written as

$$\begin{aligned}
\dot{m}_1 &= \beta_1 - \delta_1 m_1 + K_{m_1,u}u_1 \\
\dot{m}_2 &= \beta_2 - \delta_2 m_2 + K_{m_2,u}u_1 \\
\dot{p}_1 &= R^{\text{tot}} \frac{\frac{m_1}{K_{M,1}}}{1 + \sum_{j=1}^{n} \frac{m_j}{K_{M,j}}} - \delta p_1 \\
\vdots &= \qquad \vdots \\
\dot{p}_n &= R^{\text{tot}} \frac{\frac{m_n}{K_{M,n}}}{1 + \sum_{j=1}^{n} \frac{m_j}{K_{M,j}}} - \delta p_n \\
\dot{m}_3 &= \beta_3 - \delta_3 m_3 \\
\vdots &= \qquad \vdots \\
\dot{m}_n &= \beta_n - \delta_n m_n.
\end{aligned}$$

Let us examine what happens if we introduce only ribosomal loading on translation of mRNA into protein. Here we have assumed that binding of the ribosomal machinery to the ribosome binding site of an mRNA molecule happens much faster and that the ribosomal translational complex satisfies a Michaelis-Menten assumption, i.e. it reaches steady state much faster than $m_1, ..m_n, p_1, ..., p_n$.

To investigate the existence of a right half plane zero, we calculate the Jacobian in equation (13) for some nominal equilibrium point x_e, and define the block elements of the the Jacobian J as

$$J \equiv \left[\begin{array}{c|c} A_{11}(x_e) & A_{12}(x_e) \\ \hline A_{21}(x_e) & A_{22}(x_e) \end{array}\right]$$

with

$$B = \begin{bmatrix} K_{m_1,u} & K_{m_2,u} & 0 & \dots & 0 \end{bmatrix}^T$$

and

$$C = \begin{bmatrix} 0 & 0 & 1 & 0 \dots & 0 \end{bmatrix}.$$

Notice that the signed Boolean structure of A_{11} is identical to the signed Boolean structure of the A matrix in the IFFL system (16). Following the pattern discovered in the above example, if we suppose

$$\frac{\frac{m_{j,e}}{K_{M,j}}}{\left(\frac{m_{2,e}}{K_{M,2}}\right)^2} = O(\epsilon) \text{ for } j \neq 2 \; ; \; n = O(1) \tag{14}$$

then a direct application of the Woodbury matrix identity,

$$\left[\begin{array}{ccc|ccc|ccc}
-\delta_1 & 0 & 0 & 0 & \dots & 0 & 0 & \dots & 0 \\
0 & -\delta_2 & 0 & 0 & \dots & 0 & 0 & \dots & 0 \\
\frac{R^{\text{tot}}}{K_{M,1}}\frac{\left(\sum_{j\neq 1}\frac{m_{j,e}}{K_{M,j}}+1\right)}{\left(1+\sum_j \frac{m_{j,e}}{K_{M,j}}\right)^2} & -\frac{R^{\text{tot}}}{K_{M,2}}\frac{m_{1,e}}{K_{M,1}}\frac{1}{\left(1+\sum_j \frac{m_{j,e}}{K_{M,j}}\right)^2} & -\delta & 0 & \dots & 0 & -\frac{R^{\text{tot}}}{K_{M,3}}\frac{m_{1,e}}{K_{M,1}}\frac{1}{\left(1+\sum_j \frac{m_{j,e}}{K_{M,j}}\right)^2} & \dots & -\frac{R^{\text{tot}}}{K_{M,n}}\frac{m_{1,e}}{K_{M,1}}\frac{1}{\left(1+\sum_j \frac{m_{j,e}}{K_{M,j}}\right)^2} \\
\hline
-\frac{R^{\text{tot}}}{K_{M,1}}\frac{m_{2,e}}{K_{M,2}}\frac{1}{\left(1+\sum_j \frac{m_{j,e}}{K_{M,j}}\right)^2} & \frac{R^{\text{tot}}}{K_{M,2}}\frac{\left(1+\sum_{j\neq 2}\frac{m_{j,e}}{K_{M,j}}\right)}{\left(1+\sum_j \frac{m_{j,e}}{K_{M,j}}\right)^2} & 0 & -\delta & \dots & 0 & -\frac{R^{\text{tot}}}{K_{M,3}}\frac{m_{2,e}}{K_{M,2}}\frac{1}{\left(1+\sum_j \frac{m_{j,e}}{K_{M,j}}\right)^2} & \dots & -\frac{R^{\text{tot}}}{K_{M,n}}\frac{m_{2,e}}{K_{M,2}}\frac{1}{\left(1+\sum_j \frac{m_{j,e}}{K_{M,j}}\right)^2} \\
\vdots & \vdots & \vdots & \vdots & \vdots & \vdots & \vdots & \vdots & \vdots \\
-\frac{R^{\text{tot}}}{K_{M,1}}\frac{m_{n,e}}{K_{M,n}}\frac{1}{\left(1+\sum_j \frac{m_{j,e}}{K_{M,j}}\right)^2} & -\frac{R^{\text{tot}}}{K_{M,2}}\frac{m_{n,e}}{K_{M,n}}\frac{1}{\left(1+\sum_j \frac{m_{j,e}}{K_{M,j}}\right)^2} & 0 & 0 & \dots & -\delta & -\frac{R^{\text{tot}}}{K_{M,3}}\frac{m_{n,e}}{K_{M,n}}\frac{1}{\left(1+\sum_j \frac{m_{j,e}}{K_{M,j}}\right)^2} & \dots & -\frac{R^{\text{tot}}}{K_{M,n}}\frac{\left(1+\sum_{j\neq n}\frac{m_j}{K_{M,j}}\right)}{\left(1+\sum_j \frac{m_{j,e}}{K_{M,j}}\right)^2} \\
0 & 0 & 0 & 0 & \dots & 0 & -\delta_3 & \dots & 0 \\
\vdots & \vdots & \vdots & \vdots & \vdots & \vdots & \vdots & \vdots & \vdots \\
0 & 0 & 0 & 0 & \dots & 0 & 0 & \dots & -\delta_n
\end{array}\right] \tag{13}$$

allows us to write the transfer function as $G(s)$

$$\begin{aligned}
&= C\left(\left[\begin{array}{c|c} sI - A_{11}(x_e) & -A_{12}(x_e) \\ \hline -A_{21}(x_e) & sI - A_{22}(x_e) \end{array}\right]^{-1}\right) B \qquad (15)\\
&= C\left[\begin{array}{c|c} \left(sI - A_{11} - A_{12}(sI - A_{22})^{-1}A_{21}\right)^{-1} & \star \\ \hline \star & \star \end{array}\right] B \\
&= \begin{bmatrix}0\\0\\1\end{bmatrix}^T \left((sI - A_{11}) - A_{12}(sI - A_{22})^{-1}A_{21}\right)^{-1} \begin{bmatrix}K_{m_1,u}\\K_{m_2,u}\\0\end{bmatrix}
\end{aligned}$$

and since $1 >> \epsilon$, if we pull out $(m_2/K_{M,2})^2$ from the denominator in A_{12}, A_{21}, and A_{22} it is easy to see that A_{12} is $O(\epsilon)$ and A_{21}, A_{22} is at most $O(1)$, thus implying that

$$\left((sI - A_{11}) - A_{12}(sI - A_{22})^{-1}A_{21}\right)^{-1} \approxeq (sI - A_{11})^{-1}.$$

Next, note that the signed Boolean structure of (A_{11}, B_1) is of the form

$$\left(\begin{bmatrix} -\alpha_{m_1} & 0 & 0 \\ 0 & -\alpha_{m_2} & 0 \\ K_{p_1,m_1} & -K_{p_1,m_2} & -\alpha_{p_1} \end{bmatrix}, \begin{bmatrix} K_{m_1 u} \\ K_{m_2 u} \\ 0 \end{bmatrix}\right) \tag{16}$$

Permuting the states, so that p_1 is x_O and m_2 is x_I and $(u - u_e)$ is u, and applying the equations in (12) we get $W_{II}(s) = -\alpha_{m_2}, V_I(s) = K_{m_2 u}, W_{OO}(s) = -\alpha_{p,1}$ and

$$\begin{aligned} W_{OI}(s) &= -K_{p_1,m_2} \\ V_O(s) &= \frac{K_{p_1,m_1}K_{m_1 u}}{s + \alpha_{m_1}} \end{aligned}$$

and $f(x) = -\alpha_{m_2} - \left(-\frac{K_{p_1,m_2}K_{m_2,u}}{K_{p_1,m_1}K_{m_1,u}}(s + \alpha_{m_1})\right)$ In this case, notice that the incoherence in K_{p_1,m_2} and K_{p_1,m_1} determines the sign of $\frac{W_{OI}(x)V_I(x)}{V_O(x)} \leq 0$ Also, $f(x)$ has relative degree -1 and the condition that $0 \leq K < 1$ implies that

$$K_{p_1,m_2}K_{m_2,u} < K_{p_1,m_1}K_{m_1,u} \tag{17}$$

and if

$$\left(\frac{K_{p_1,m_2}K_{m_2,u}}{K_{p_1,m_1}K_{m_1,u}}(\alpha_{m_1})\right) > \alpha_{m_2} \tag{18}$$

then $f(x) \geq 0$ for all nonnegative real x and by Theorem 1 the system will have a right half plane zero.

In this particular class of systems, we assume degradation is not substantially saturated, i.e. we can approximate each degradation rate as linear. The reader will find that if an input-coupled system is posed with degradation crosstalk as the sole source of crosstalk, the system will have the potential to possess a right half plane zero only if 1) there is a down-regulation of one gene by another, and 2) a third gene dominates use of the degradation enzymes, so much that it sequesters the enzymes from the first or second. The key is the introduction of an incoherent feedforward loop in the system. When there are multiple sources of resource-mediated crosstalk, again, multiple feedforward loops will be present and a right half plane zero will be present if the dominant feedforward loop is an incoherent feedforward loop.

V. ClpXP Loading and Implications on the σ^{38} (RpoS) Regulated Stress Response

In this section we show how loading effects introduced by two competing pathways: 1) a pathway that is introduced synthetically with strong production gain and degradation gain and 2) the stress response pathway regulated by the master stress response regulator σ^{38} (RpoS) results in an incoherent feedforward loop with the potential for a right half plane zero. Specifically, we consider the effects of adding a high copy number gene that is engineered to have an LVA tag [4], a standard modification tag added to proteins to tune degradation rates. However, since ClpXP degrades σ^{38} and any LVA-tagged molecule, when LVA-tagged proteins are produced in high quantity by a high copy number gene, the result is a sudden increase in ClpXP degradable proteins which can lead to ClpXP saturation [13]. ClpXP regulates σ^{38} concentration, so if enough ClpXP is sequestered, the result is that the effective lifetime of a σ^{38} molecule is extended. Furthermore, σ^{38} is the master stress response (up)regulator, an increase in its lifetime results in activation of critical stress response genes. These stress response genes can have adverse effects on cell metabolism, unnecessarily tax transcriptional and translational machinery (e.g. HPI and HPII catalases [14] which convert toxic hydrogen peroxide molecules into hydrogen and water), or in the worst case, induce cell lysis (e.g. the protein entericidin which induces cell lysis [15]).

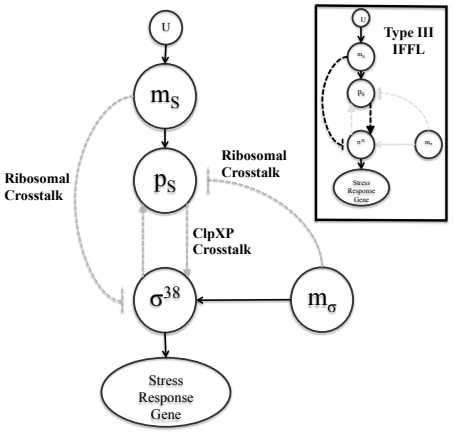

Fig. 3. A diagram illustrating the interactions between chemical species in system (19). A synthetic gene is induced by a small molecule u, resulting in expression of mRNA molecule m_S. m_S translates into LVA-tagged protein p_S-LVA. The m_S mRNA molecules sequester ribosomes from m_σ, the mRNA transcript for σ^{38} — this creates a crosstalk interaction where m_S effectively down regulates σ^{38} expression (similarly, m_σ down regulates p_S expression, but only weakly when the synthetic gene is at high copy number). The p_S protein sequesters ClpXP from σ^{38}, — this creates a crosstalk interaction where p_S in effect extends the lifetime of σ^{38}, which we indicate with an up-regulation arrow from p_S to σ^{38}. The inset highlights the Type III incoherent feedforward loop [12] is introduced via ribosomal and ClpXP sequestration interactions. The relevant crosstalk interaction arrows in the IFFL are drawn as dotted and a darker color than the other crosstalk interactions.

While there are certain scenarios where inducing cell death may be the goal of a synthetic circuit, it is often the goal to engineer biocircuits that do not adversely impact the health of its host or minimally perturb the activity of host housekeeping genes. Therefore, it is important to understand whether such a synthetic circuit can adversely affect the cell's ability to regulate its stress response. A schematic illustrating the interactions of the circuit, including the indirect crosstalk interactions (dotted) is shown in Figure 3. We model the system as follows:

$$
\begin{aligned}
\dot{m}_S &= P^{\text{tot}} k^p_{\text{cat}} \frac{N\frac{D_S}{K_{M,D}}}{1+N\frac{D_S}{K_{M,D}}+\frac{D_\sigma}{K_{M,\sigma_D}}} - \delta_S m_s + k_{su}u,\\
\dot{m}_\sigma &= P^{\text{tot}} k^p_{\text{cat}} \frac{\frac{D_\sigma}{K_{M,\sigma_D}}}{1+N\frac{D_S}{K_{M,D}}+\frac{D_\sigma}{K_{M,\sigma_D}}} - \delta_\sigma m_\sigma, \qquad (19)\\
\dot{p_S} &= k_{\text{cat}} \frac{R^{\text{tot}}\frac{m_s}{K_{M,s}}}{1+\frac{m_s}{K_{M,S}}+\frac{m_\sigma}{K_{M,\sigma}}} - \kappa_{\text{cat}} \frac{C^{\text{tot}}\frac{P_S}{\kappa_{M,S}}}{1+\frac{P_s}{\kappa_{M,S}}+\frac{\sigma^{38}}{\kappa_{M,\sigma}}},\\
\dot{\sigma^{38}} &= k_{\text{cat}} \frac{R^{\text{tot}}\frac{m_\sigma}{K_{M,\sigma}}}{1+\frac{m_\sigma}{K_{M,\sigma}}+\frac{m_S}{K_{M,S}}} - \kappa_{\text{cat}} \frac{C^{\text{tot}}\frac{\sigma^{38}}{\kappa_{M,\sigma}}}{1+\frac{P_s}{\kappa_{M,S}}+\frac{\sigma^{38}}{\kappa_{M,\sigma}}},\\
\dot{x}_{stress} &= \alpha\frac{\sigma^{38}}{k_M+\sigma^{38}} - \delta_x x_{stress}\,.
\end{aligned}
$$

The Jacobian of the system has the following form:

$$
\begin{bmatrix}
-a_{11} & 0 & 0 & 0 & 0\\
0 & -a_{22} & 0 & 0 & 0\\
a_{31} & -a_{32} & -a_{33} & a_{34} & 0\\
-a_{41} & a_{42} & a_{43} & -a_{44} & 0\\
0 & 0 & 0 & a_{54} & -a_{55}
\end{bmatrix},
$$

with $B = \begin{bmatrix} k_{su} & 0 & 0 & 0 & 0 \end{bmatrix}^T$, where a_{ij} are computed in the usual fashion. Notice, the definition of the transfer function depends on which state we choose as our output. Since we are considering the copy number of our circuit to be particularly large, e.g. if the circuit was implemented on a high copy plasmid, then our concern is how drawing from the resources of the cell affects a critical survival mechanism — the stress response pathway. Thus, we are interested in how inducing our synthetic pathway with u affects production of stress response protein x_{stress}. Here x_{stress} can be interpreted as any of the proteins typically (positively) regulated by σ^{38}, e.g. Thus, if u renders the cell unable to respond to stress, or worse yet, indirectly activates the stress response, this could lead to poor performance of the synthetic circuit or in the worst case, destruction of the host via cell lysis.

Computing the transfer function gives

$$
G(s) = \frac{(-a_{41}a_{54}k_{su})\left(s - \frac{a_{43}a_{31}}{a_{41}} + a_{33}\right)}{D(s)}
$$

where $D(s) = (s+a_{55})(a_{33}a_{44} - a_{34}a_{43} + a_{33}s + a_{44}s + s^2)(s+a_{11})$ and the zero can be written simply as

$$
z = \frac{a_{54}a_{43}a_{31}k_{su}}{a_{54}a_{41}k_{su}} - a_{33} = \frac{k_{\text{cat}}C^{\text{tot}}\left(\frac{\sigma^{38}_e}{\kappa_{M,\sigma}}\frac{K_{M,\sigma}}{m^e_\sigma} - 1\right)}{\left(1+\frac{p^e_s}{\kappa_{M,s}}+\frac{\sigma^{38}_e}{\kappa_{M,\sigma}}\right)^2}
$$

which is positive if $\frac{K_{M,\sigma}}{m^e_\sigma} - \frac{\kappa_{M,\sigma}}{\sigma^{38}_e} > 0$. Examining the first expression for z, we see that the system has a right half plane zero if the effective gain of "up-regulation" of σ^{38} via Clp-XP saturation ($a_{43}a_{31}k_{su}$), normalized by the effective gain of "down-regulation" of σ^{38} via ribosomal loading ($a_{41}k_{su}$) is sufficiently large, specifically to exceed the rate of degradation of p_S (a_{33}). When overall up-regulation of σ^{38} only slightly exceeds degradation of σ^{38}, the result is a particularly slow right half plane zero.

Copy number of the synthetic circuit also plays a role in determine the size of z. When z is positive and small, increasing the copy number N in system (19) increases m^e_s which results in an increase in p^e_s. Notice that increasing p^e_s also results in a decrease in σ^{38}_e. If $z > 0$, then increasing copy number N drives z towards 0, resulting in a slower settling time and larger amplitude of the inverse transient. We consider the average copy numbers N of 4 standard vectors that are used to carry synthetic circuits in *E. coli* and plot the step response as a function of N (Figure 4). If we apply the Bode integral formula for the complementary sensitivity function $T(s)$, we obtain the following lower bound:

$$
\int_0^\infty \log|T(j\omega)|d(\frac{1}{\omega}) \geq \frac{\left(1+\frac{p^e_s}{\kappa_{M,s}}+\frac{\sigma^{38}_e}{\kappa_{M,\sigma}}\right)^2}{k_{\text{cat}}C^{\text{tot}}\left(\frac{\sigma^{38}_e}{\kappa_{M,\sigma}}\frac{K_{M,\sigma}}{m^e_\sigma} - 1\right)}
$$

Since the error in tracking is $E(s) = S(s)(R(s) - D(s)) + T(s)M(s)$, then $T(s)$ is a measure of how uncertainty in measurements, or measurement noise, is amplified to error. However, the issue is not about control performance or trajectory tracking (though that may be the case in a synthetic

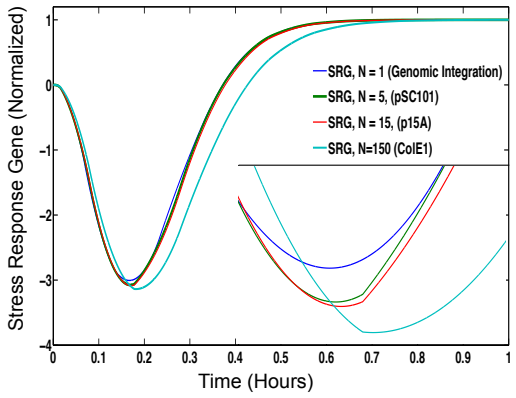

Fig. 4. Normalized step response curves of stress response gene x_{stress} for the nonlinear system (19) plotted as a function of time and the synthetic gene copy number N. We selected average values representative of low, medium and high copy numbers of plasmid (displayed with a standard ORI of that copy number). These curves were generated using the following parameters: $P^{\text{tot}} = 200$ nM, $R^{\text{tot}} = 80$ nM, $C^{\text{tot}} = 75$ nM, $D_s = D_\sigma = 1$ nM, $k^p_{\text{cat}} = .009$ /s, $k_{\text{cat}} = \kappa_{\text{cat}} = .0002$ /s, $K_{M,S} = K_{M,\sigma} = K_{M,D} = K_{M,\sigma_D} = 500$ nM , $\kappa_{M,S} = \kappa_{M,\sigma} = 3$ nM, $\delta_S = \delta_\sigma = \delta_x = 5\times10^{-3}$ /s, $\alpha = 10$ nM/s, $k_M = 30$ nM, $k_{su} = .0001$ /s. A step of 1 nM was used. (Inset) A magnified view of the trough in the inverse transient of the step response.

system using *in silico* control approaches [16]). The relevant goal is to implement synthetic pathways in biology that do not jeopardize the health of the cell or unintentionally activate unnecessary pathways.

However, when we use ClpXP to mediate degradation in our synthetic circuit, a right half plane zero is introduced into the system, resulting in significant coupling to the stress response genes of the cell. Further, induction of our synthetic circuit results in 1) a transient (inverse) dynamic wherein the cell loses its ability to respond to stress, 2) the eventual up-regulation of stress response genes whether or not there actually is environmental stress. Both of these outcomes can be deleterious to the cell.

In presenting this example, our purpose is to simply increase understanding of the *potentially* adverse consequences of introducing LVA-tagged molecules on a high copy number biocircuit. We do not claim that right half plane zeros will always exist for such biocircuits, as the existence of the right half plane zero is strongly dependent on the equilibrium values of the chemical species involved, the Michaelis-Menten constants, and the amount of ribosomes, polymerases, and ClpXP in each cell. Thus, our results should be viewed as an additional consideration when using ClpXP to control degradation rates.

VI. Conclusion

In this work we reviewed the principle of resource loading and examined its effects on a signal cascade that implemented repression. We showed that saturation and competition of degradation enzymes produces unintended crosstalk interactions. Those crosstalk interactions introduced an incoherent feedforward loop, and under certain parametric conditions, a right half plane zero in the local dynamics of an equilibrium point. We analyzed the incoherent feedforward loop using a simple example and derived sufficient conditions for a multi-dimensional SISO system to have an incoherent feedforward loop and additionally, a right half plane zero. We then applied this result to derive parametric conditions under which a class of transcription-translation systems and a synthetic system leveraging LVA degradation technology would have a right half plane zero. We stress that cells always deal with finite resources [17] and as shown in [4], expressing just two genes was already enough to completely saturate ClpXp using typical promoters (pTet and pAra). It is thus likely that for any reasonably sized circuit, that the resources for either production or degradation machinery will be saturated. Therefore, the issue of of characterizing how right half plane zeros arise from resource limitations is an important area to explore for understanding the limits of controllability in synthetic (and even naturally occurring) circuits.

References

[1] J. Stricker et al, "A fast, robust, and tunable synthetic gene oscillator", *Nature*, vol. 456, no. 7221, pp. 516–519, 2008.

[2] M. B. Elowitz and S. Leibler, "A synthetic oscillatory network of transcriptional regulators", *Nature*, vol. 403, no. 6767, pp. 335–338, 2000.

[3] L. Qi et al, "Rna processing enables predictable programming of gene expression", *Nature Biotechnology*, vol. 30, no. 10, pp. 1002–1006, 2012.

[4] N. Cookson et al, "Queueing up for enzymatic processing: correlated signaling through coupled degradation", *Molecular Systems Biology*, vol. 7, no. 561, 2011.

[5] D. Del Vecchio, A. J. Ninfa, and E. D. Sontag, "Modular cell biology : retroactivity and insulation", *Mol. Syst. Biol*, vol. 4, pp. 161, 2008.

[6] E. Yeung, J. Kim, Y. Yuan, J. Goncalves, and R. Murray, "Quantifying crosstalk in biochemical systems", *The Proceedings of the 49th IEEE Conference on Decision and Control*, December 2012.

[7] D. Siegal-Gaskins, V. Noireaux, and R. M. Murray, "Biomolecular resource utilization in elementary cell-free gene circuits", *The Proceedings of the IEEE American Control Conference, to appear*, June 2013.

[8] S. Jayanthi and D. Del Vecchio, "Tuning genetic clocks employing dna binding sites", *PLoS ONE*, vol. 7, no. 7, pp. e41019, 07 2012.

[9] K. Zhou J. Doyle, K. Glover, *Robust and Optimal Control*, Prentice Hall, Englewood Cliffs, N.J., 1996.

[10] F. A. Chandra., G. Buzi, and J. C. Doyle., "Glycolytic oscillations and limits on robust efficiency", *Science*, vol. 333, no. 6039, pp. 187–192, 2011.

[11] J. Gonçalves, R. Howes, and S. Warnick, "Dynamical structure functions for the reverse engineering of LTI networks", *IEEE Transactions of Automatic Control, 2007*, August 2007.

[12] S. Mangan and U. Alon, "Structure and function of the feed-forward loop network motif", *Proceedings of the National Academy of Sciences*, vol. 100, no. 21, pp. 11980–11985, 2003.

[13] A. Fredriksson, M. Ballesteros, C. N Peterson, Ö Persson, T. J. Silhavy, and T. Nyström, "Decline in ribosomal fidelity contributes to the accumulation and stabilization of the master stress response regulator σs upon carbon starvation", *Genes & development*, vol. 21, no. 7, pp. 862–874, 2007.

[14] P. C. Loewen, B. Hu., J. Strutinsky., and R. Sparling, "Regulation of the rpos regulon of escherichia coli", *Canadian Journal of Microbiology*, vol. 44, pp. 707–717, 1998.

[15] R. E. Bishop, B. K. Leskiw, R. S. Hodges, C. M. Kay, and J. H. Weiner, "The entericidin locus of escherichia coli and its implications for programmed bacterial cell death", *Journal of Molecular Biology*, vol. 280, no. 4, pp. 583 – 596, 1998.

[16] A. Milias-Argeitis, S. Summers, J. Stewart-Ornstein, I. Zuleta, D. Pincus, H. El-Samad, M. Khammash, and J. Lygeros, "In silico feedback for in vivo regulation of a gene expression circuit", *Nature biotechnology*, 2011.

[17] M. Scott, C.W. Gunderson, E. M. Mateescu, Z. Zhang, and T. Hwa, "Interdependence of cell growth and gene expression: Origins and consequences", *Science*, vol. 330, no. 6007, pp. 1099–1102, 2010.